Available online at www.sciencedirect.com
SCIENCE DIRECT®
Journal of Sound and Vibration 296 (2006) 602–622
JOURNAL OF SOUND AND VIBRATION
www.elsevier.com/locate/jsvi

Diversion of energy flow near crack tips of a vibrating plate using the structural intensity technique

H.P. Lee[a,b,*], S.P. Lim[a], M.S. Khun[a]

[a]Department of Mechanical Engineering, National University of Singapore, 9 Engineering Drive 1, Singapore 117576, Singapore
[b]Institute of High Performance Computing, 1 Science Park Road, #01-01 The Capricorn, Singapore Science Park II, Singapore 117528, Singapore

Received 13 September 2004; received in revised form 13 February 2006; accepted 4 March 2006
Available online 12 May 2006

Abstract

The structural intensity (SI) of a vibrating rectangular plate with a crack is computed using the finite element method. The overall behavior of power flow patterns of the cracked plate is investigated. The presence of the crack can be identified by the changes of the directions of SI vectors near the crack. The effects of orientation of the crack and crack length on the energy flow pattern are also investigated. The SI method is then used to explore the positioning of dampers in vibrating thin plates to divert the vibration energy flow away from crack tips. This approach is proposed as a temporary measure to prevent further propagation of the crack before repair of the crack can be done.

1. Introduction

It has been known that the presence of a flaw or local defect in structural elements leads to changes in local flexibility. The structural characteristics affected by fatigue initiated cracks or manufacturing defects result in non-predictable, or even disastrous structural responses. Thus, the understanding of the dynamic behavior of cracked structures and crack detection and monitoring methods are the focus of numerous studies. A large amount of literature is available relating to the stress intensity factor at the crack tip. However, only a limited numbers of papers are related to the vibration related damage diagnoses of plate structures.

A damage detection vibration analysis to predict the location and depth of crack in a rectangular plate was carried out by Khadem and Rezaee [1]. A comprehensive review on the literature of the vibration of cracked structures was made by Dimarogonas [2]. The influence of cracks on the natural frequency of the plate has been investigated in Refs. [3–6]. Stahl and Keer [3] determined the natural frequencies and stability of the cracked plates by using the homogeneous Fredholm integral equation of the second kind. Lee [4] investigated the fundamental frequencies of annular plates with internal cracks using the Rayleigh method. The vibration of a rectangular plate with a parallel crack on one edge was studied by Solecki [5]. Krawczuk et al. [6] included

*Corresponding author. Institute of High Performance Computing, 1 Science Park Road, #01-01 The Capricorn, Singapore Science Park II, Singapore 117528, Singapore. Tel.: +65 6419 1303; fax: +65 6419 1480.
E-mail address: hplee@ihpc.a-star.edu.sg (H.P. Lee).

0022-460X/$ - see front matter
doi:10.1016/j.jsv.2006.03.007

the effect of plasticity at the crack tip in modeling a crack plate. However, they showed that the effect of plasticity on the natural frequency could be neglected.

The structural power flow or structural intensity (SI) was introduced by Noiseux [7], Pavic [8], Verheij [9] and Hambric [10] to solve structural borne sound problems. Vibration of an elastic structure induces the propagation of vibratory energy through the structure and it is called vibrational or structural power flow. SI is defined as the instantaneous rate of energy transfer per unit area. The SI field indicates the magnitude and direction of vibratory energy flows at any point of a structure. The SI analysis of a simply supported plate was carried out by Gavric [11] using the finite element method (FEM). The SI approach was employed to compute the surface mobility of a thin plate by Li and Lai [12]. Li et al. [13] proposed the diagnosis of flaws at structural members using vibrational power flow. A defective periodic beam structure was studied and the position and size of the flaw can be identified using the structural power flow. Recently, the SI techniques was also used for computing the vibration energy flow pattern of plates with multiple cutout by Khun et al. [14], composite plates with holes, rotating hard disk and designing of stiffened plates in marine structures [15–17].

In order to model the cracked structures, the singular elements or special elements at the crack tip are preferred [2,5] if the behavior of the crack is under investigation. There are numerous ways to model the crack tip to obtain a good result for the crack tip stress field. The use of quarter point element has been found

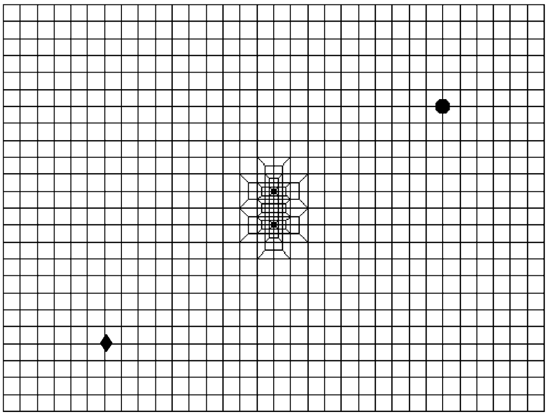

(a)

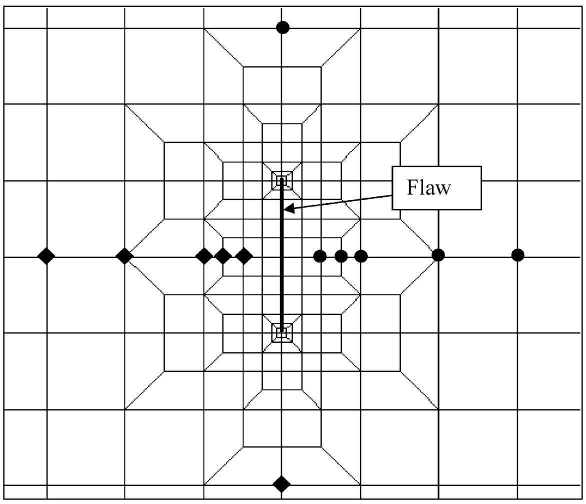

(b)

Fig. 1. (a) The basic finite element model of a cracked plate. (b) A higher density FE meshes around the crack and showing the positions of the source by '◆' and the sink by '●' for Figs. 6(a)–(e) and 7.

in Refs. [18,19] and this method is preferred in the finite element modeling because of its accuracy and simplicity.

However, for the users of general purpose finite element programs, a more convenient approach is to increase the mesh density at the crack region [20]. Malone et al. [20] used triangular linear elements to predict the vertical displacement and stress intensity factor of an infinite plate. The sizes of elements were increased for regions approaching the crack tip. Vafai and Estenkanchi [21] carried out a parametric study using four-noded shell elements on cracked plates and shells. Stress and displacement fields were predicted by a high order of mesh refinement at the crack tip with no singular or special elements.

The *h*-order mesh refinement at the crack front can be used to predict the overall stress and displacement with acceptable precision [20,21]. It was found that there was no difference in moment distribution of cracked plates modeled with and without crack tip singularity [3]. In this study, the SI of the plate affected by the presence of a crack is studied. The FEM is used to compute the SI of the cracked plate structure. The SI technique is employed to investigate the changes of structural characteristics caused by the crack-like defects which result in the changes of energy flow pattern of SI near the cracks. A higher order mesh refinement is used at the crack tip region. The SI method is then used to explore the positioning of dampers in vibrating thin plates to divert the vibration energy flow away from crack tips. This approach is proposed as a temporary measure to prevent the further propagation of the crack before repair of the crack can be done.

2. Structural intensity of a plate

Vibrational power flow per unit area of a dynamically loaded structure is defined as the SI. The net energy flow through the structure is the time average of the instantaneous intensity and the intensity at a point in the *i*-direction can be defined as [11]

$$I_i = \langle I_i(t) \rangle = \langle -\sigma_{ij}(t) v_j(t) \rangle, \quad i,j = 1,2,3,$$

where $\sigma_{ij}\,(t)$ and $v_j\,(t)$ are the stress and velocity, respectively, in the *j*-direction at time *t*.

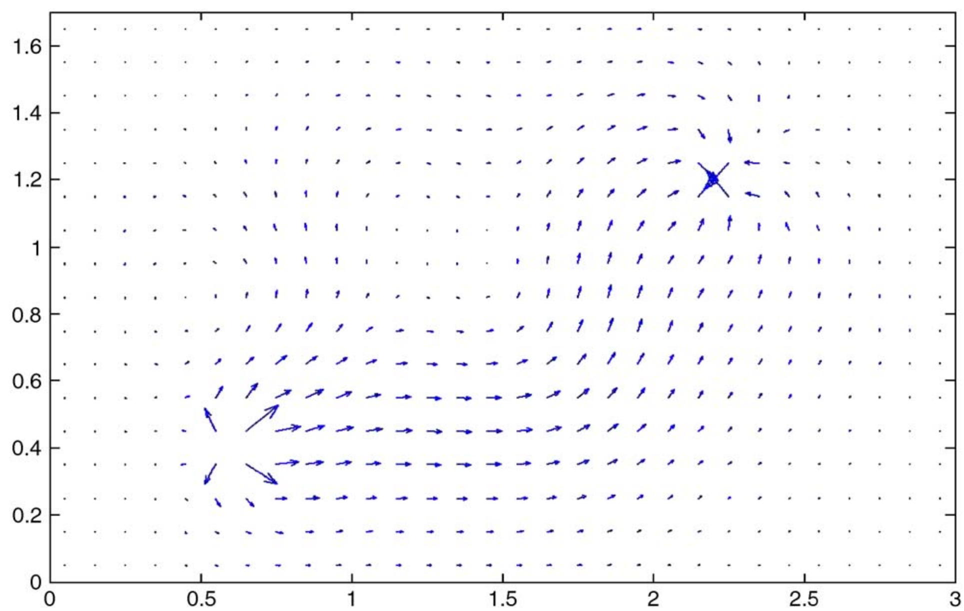

Fig. 2. Structural intensity of a simply supported rectangular plate with an attached damper (50 Hz).

For the flexural vibration of a plate, the intensity in the x-direction can be expressed in terms of the out of plane displacement w as

$$P_x = D\left[\frac{\partial(\nabla^2 w)}{\partial x}\,\dot{w} - \left(\frac{\partial^2 w}{\partial x^2} + v\,\frac{\partial^2 w}{\partial y^2}\right)\frac{\partial \dot{w}}{\partial x} - (1-v)\frac{\partial^2 w}{\partial x \partial y}\,\frac{\partial \dot{w}}{\partial y}\right],$$

where ∇^2 is the Laplace operator and flexural rigidity, $D = Eh^3/12(1-v^2)$.

The intensity for the y-direction can be obtained by interchanging the subscript x and y.

Stresses and displacements are usually determined from stress results and movements of the mid-surface. Therefore, the SI in the plates and shells are also used to express in the form of power flow per unit width. Besides flexural deformations of the plate, the membrane effect is also considered in the formulation of SI for shell elements. The x and y components of the SI of a flat plate using finite shell element can be expressed as [11]

$$I_x = -(\omega/2)\mathrm{Im}[\tilde{N}_x\tilde{u}^* + \tilde{N}_{xy}\tilde{v}^* + \tilde{Q}_x\tilde{w}^* + \tilde{M}_x\tilde{\theta}_y^* - \tilde{M}_{xy}\tilde{\theta}_x^*],$$
$$I_y = -(\omega/2)\mathrm{Im}[\tilde{N}_v\tilde{v}^* + \tilde{N}_{yx}\tilde{u}^* + \tilde{Q}_y\tilde{w}^* - \tilde{M}_y\tilde{\theta}_x^* + \tilde{M}_{yx}\tilde{\theta}_y^*].$$

where $\tilde{N}_x$, $\tilde{N}_y$ and $\tilde{N}_{xy} = \tilde{N}_{yx}$ are complex membrane forces per unit width of plate; $\tilde{M}_x$, $\tilde{M}_y$ and $\tilde{M}_{xy} = \tilde{M}_{yx}$ are complex bending and twisting moments per unit width of plate; $\tilde{Q}_x$ and $\tilde{Q}_y$ are complex transverse shear forces per unit width of plate; $\tilde{u}^*$, $\tilde{v}^*$ and $\tilde{w}^*$ are complex conjugate of translational displacements in x, y and z directions; $\tilde{\theta}_x^*$ and $\tilde{\theta}_y^*$ are complex conjugate of rotational displacement about x and y directions.

3. Modeling of a cracked plate

The finite element model used in this study is a simply supported rectangular plate, 0.8×0.6 m in dimension and 7 mm in thickness as shown in Fig. 1. A through-thickness crack having a length of 5 cm is assumed to

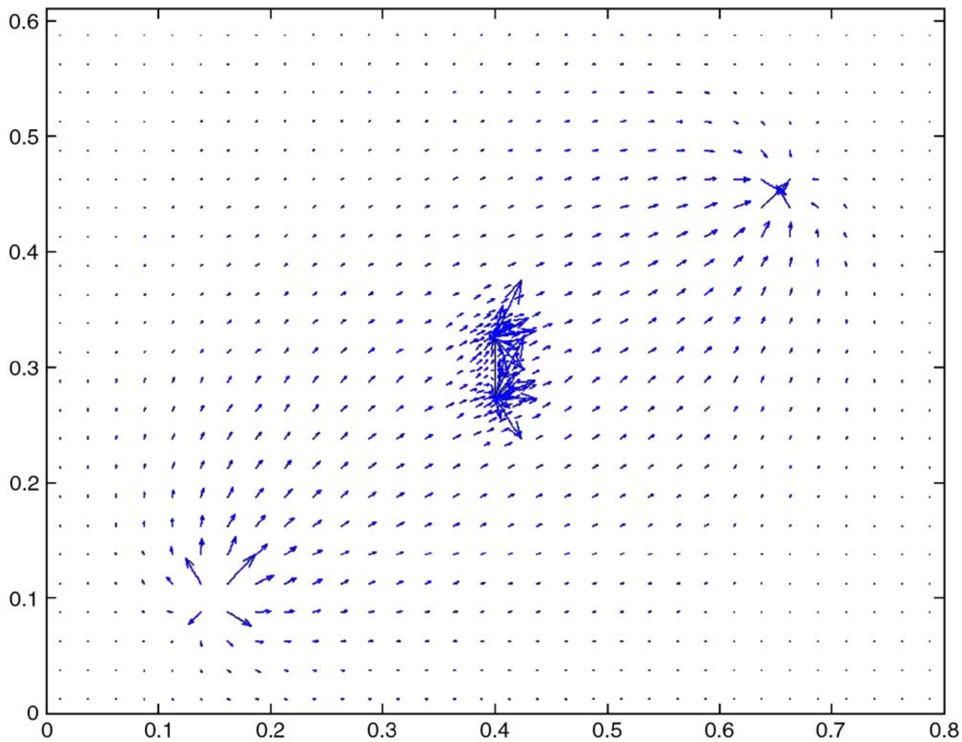

Fig. 3. Structural intensity field of the whole plate with a vertical crack (51 Hz).

present in the plate. Two different orientations of this crack, assumed to be vertical and horizontal to the length of the plate, are considered. The plate is made of steel and the properties are: Young's modulus $E = 200\,\text{GPa}$; Poisson's ratio $\nu = 0.3$ and mass density $\rho = 7850\,\text{kg/m}^3$. The amplitude and frequency of the excitation force are 200 N and 51 Hz, respectively. The viscous damper with a damping coefficient of 900 N s/m is attached to the plate. The plate is assumed to have no structural damping. The finite element meshes are refined near the crack region and a higher order mesh refinement is used at the crack tip in order to obtain sufficient accuracy of the stress and displacement predications [21] as shown in Fig. 1(b). The mesh arrangements are the same for horizontal and vertical cracks.

4. Convergence of the results

The graphical solutions of the SI fields of the flexural vibration of rectangular plate with an attached damper have been reported by Gavric and Pavic [11] and Li and Lai [12]. Gavric and Pavic [11] used the normal mode summations with the sweeping procedure to calculate the complex dynamic response of the structure. The SI at the centroids is computed using stress results at the centroids and the displacement interpolated from the nodal points. The use of commercial FEM code to computing the power flow was introduced by Hambric [10] using PATRAN. Li and Lai [12] computed the SI from the field variable using the commercial finite element software ANSYS.

In this study, the magnitudes and phase angles of the response of the flexural vibration of the plate were obtained using the finite element code ABAQUS [22]. The steady-state dynamic analysis procedure from ABAQUS [22] was employed to calculate the field variables. The eight-node quadrilateral element is used in modeling the plate. A convergence study has been carried out for calculating the SI of the plate with an attached damper. In order to examine the validity of the complex structural response results generated by Direct Solution Steady-State Dynamic Analysis in ABAQUS for computing SI, a simulation was done by employing the same as in the published results [11].

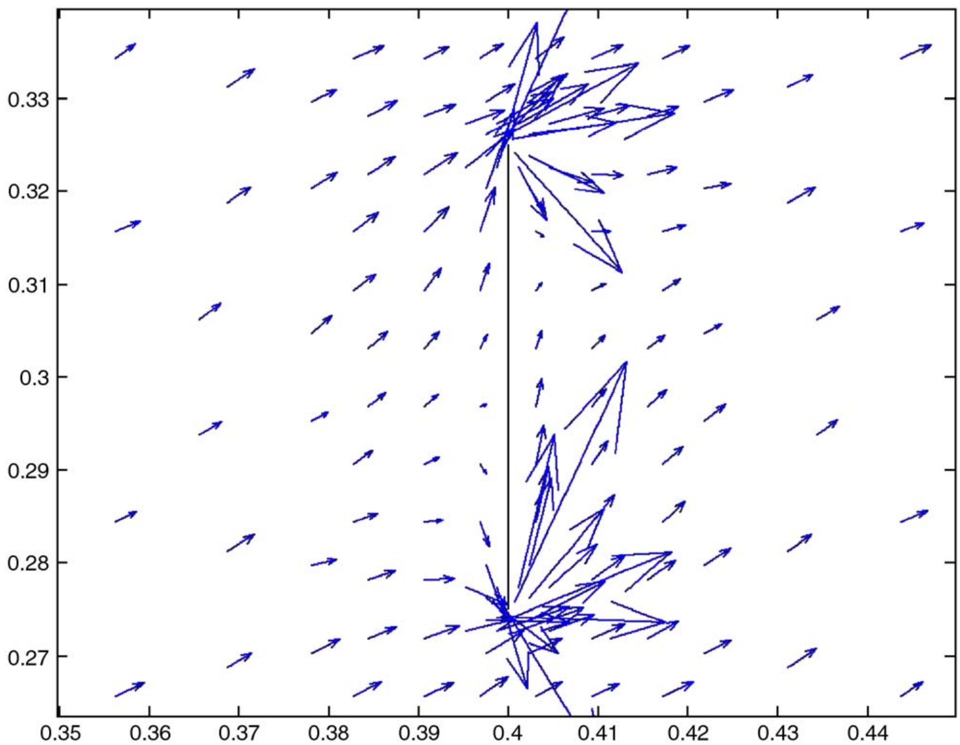

Fig. 4. Structural intensity around the vertical crack showing the changes in directions of intensity vectors at the crack edge (51 Hz).

The basic finite element model in Ref. [11] is a simply supported plate made of steel. The length and the width of the plate are 3 and 1.7 m, respectively, and the thickness of the plate is 1 cm. The material properties are taken as: Young's modulus is 2.1×10^{11} N/m^3, Poisson's ratio is 0.3 and density is 7800 kg/m^3. The plate is discretized into 510 eight-noded shell elements consisting of 1625 nodes. The sinusoidal force having a frequency of 50 Hz and a magnitude of 1000 N is applied at the coordinates of $x = 0.6$ m and $y = 0.4$ m on the plate. The structural damping is not taken into account and a dashpot with a coefficient of damping 100 N s/m is attached at the coordinates of $x = 2.2$ m and $y = 1.2$ m.

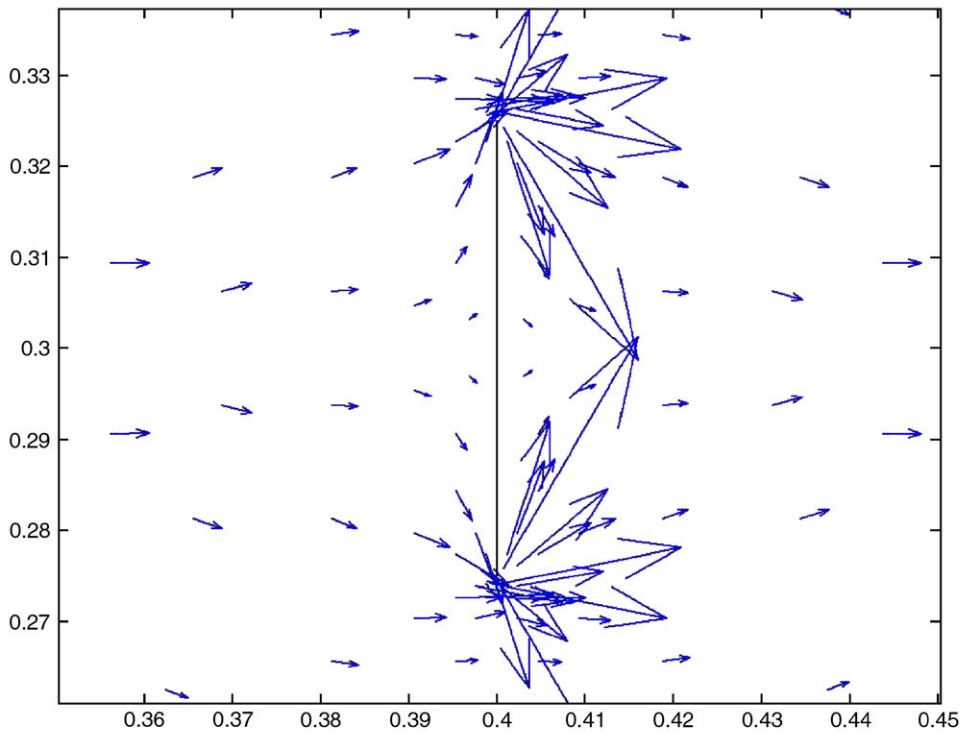

Fig. 5. Structural intensity around the crack for the model with reduced numbers of elements.

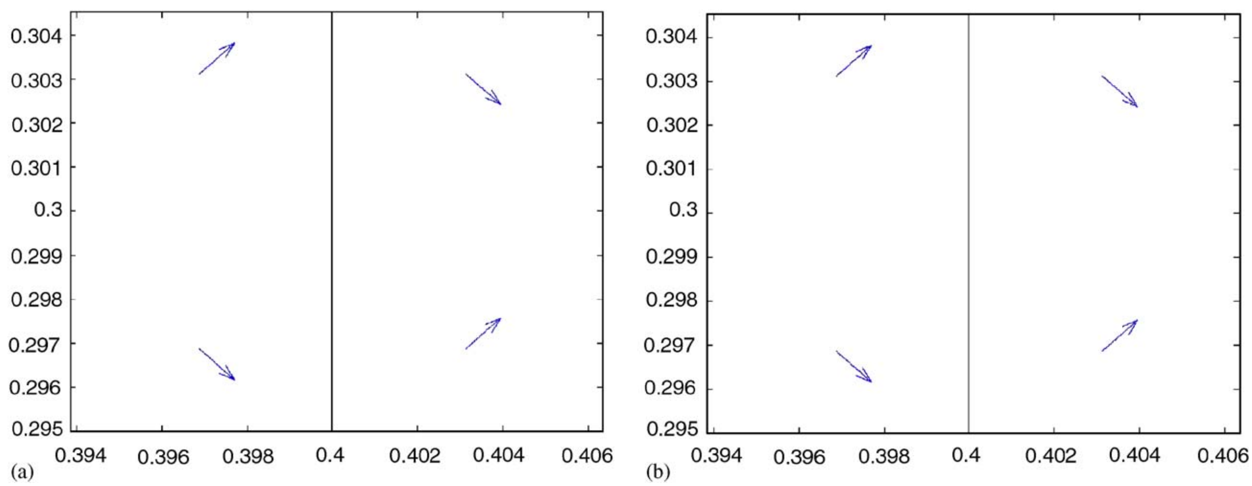

Fig. 6. Comparison of two results from two different FE models at four particular points (a) Fig. 5 and (b) Fig. 7(a).

The SI field plotted over the plate using the Direct Solution Steady-State Dynamic Procedure is shown in Fig. 2. It can be observed in the figure that the SI vectors are able to indicate the source, the sink of energy flow, and the energy flow paths between the source and the sink. The comparison of the computed results with the reported results by Gavric and Pavic [11] shows that a good agreement exists between the two results.

5. Results and discussion

5.1. Structural intensity vectors near crack tips

The SI of the plate in the vicinity of a central vertical crack has been computed and the result of SI for the whole plate is shown in Fig. 3. The excitation force is applied at $x = 0.15\,\text{m}$ and $y = 0.1\,\text{m}$ and the damper is attached at $x = 0.65\,\text{m}$ and $y = 0.45\,\text{m}$. The energy is flowing from the source to the sink smoothly in a particular path at the area in which there is no presence of crack. The region of occurrences of abrupt changes in energy pattern is observed and enlarged in Fig. 4. It can be seen in this figure that the energy flow pattern is changed near the crack boundary. When a crack is present, the intensity vectors are turned away from their normal path directing toward the discontinuous crack boundary. It implies that when the discontinuous boundary of a crack is encountered, the intensity flow direction near the crack is forced to change by the presence of the crack. After passing by the crack, it can be seen that the energy flow at the undamaged width is redistributed to all over the width. There is no power flow across the crack. The dynamic stresses and displacements of the crack tip field are complicated and so is the SI flow pattern near the crack tip. This is not of interest for the present study. The present study aims to show that the changes in the flow pattern of the SI vector near the crack is able to show the presence of the crack and therefore has the potential to be used as a crack detection technique.

In order to evaluate the accuracy of the results, another simulation has been carried using different numbers of meshes at the central region enclosing the crack. The order of mesh refinement at the crack tip remains the same order for these two cases, since the stresses may be influenced by the numbers of mesh refinements at the crack tip. The SI vectors calculated using different meshes near the crack area are plotted in Fig. 5. The elements having the same sizes at the crack boundary are used for comparison of the results. The two results with the identical simulation setup, except for different meshes and numbers of elements are shown in Fig. 6. It can be seen from the comparison that the two graphical results are in good agreement.

The occurrence of the changes of power flow pattern at a crack has also been examined by placing the vertical flaw directly between the source and the sink. The excitation force and the damper are positioned along the line of symmetry of the crack ($y = 0.3\,\text{m}$) in a manner that the crack is between them as shown in Fig. 1(b). A number of simulations have been done by moving the source and the sink closer and closer to the crack along the line joining the source and the sink. The movement for the source and the sink are equal in distance. The locations of the source and the sink in the x directions are given in Table 1 and Fig. 1(b). It can be seen from Figs. 7(a)–(e) that as the source and sink are closer to the crack edges, the changes of the direction of intensity vectors are more significant. Not only the intensity vectors near the crack boundary but also the directions of intensity vectors at the adjacent elements are changed as the source and the sink are nearer. As the source and the sink are moved closer to the crack, the intensity around the crack is increased. The next significant factor that can be observed is the changes in both the magnitudes and directions of intensity vectors at the elements closest to the crack boundary. It can be noticed that when the flow of energy

Table 1
The positions of the source and the sink along $y = 0.3\,\text{m}$ line

Figure number	The x coordinates of excitation force (m)	The x coordinates of the damper (m)
7(a)	0.35	0.475
7(b)	0.325	0.45
7(c)	0.375	0.425
7(d)	0.38125	0.41875
7(e)	0.3875	0.4125

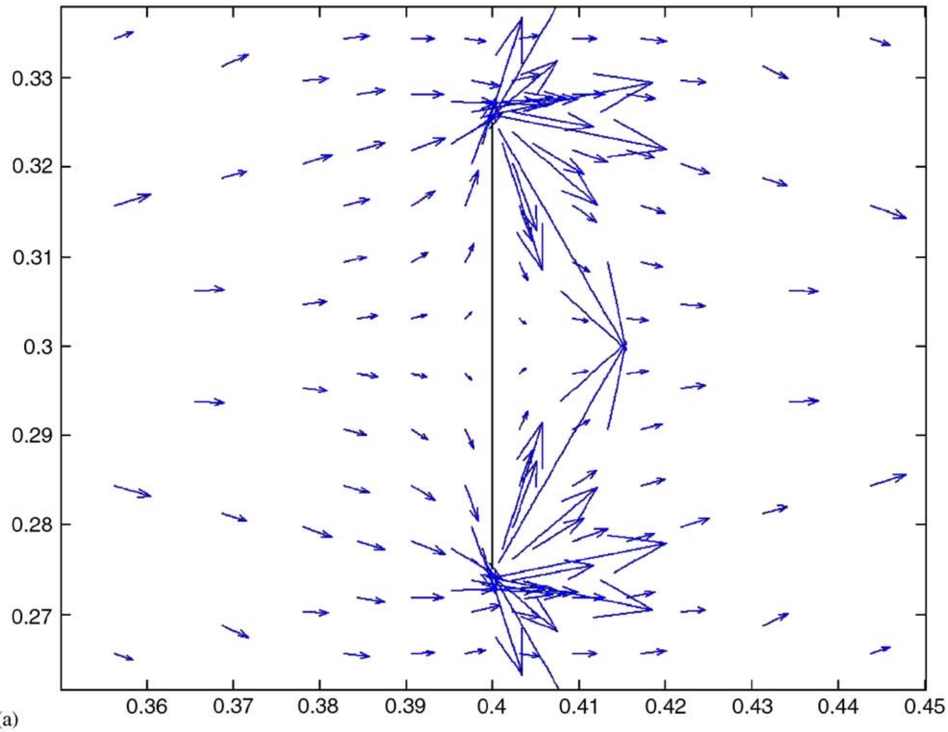

(a)

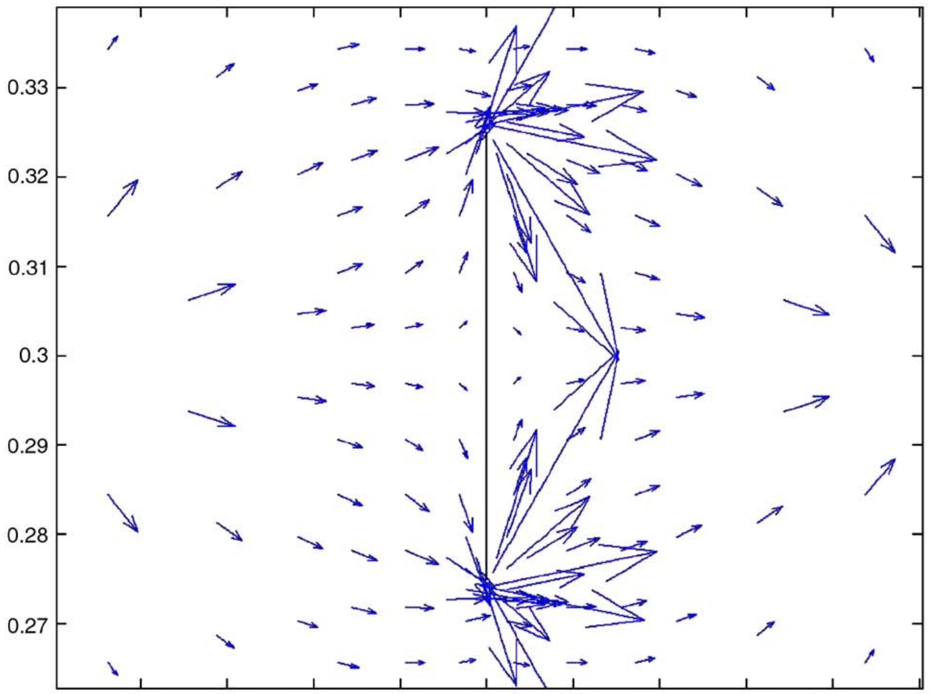

(b)

Fig. 7. Structural intensity vectors around the crack; the crack is located between the source and the sink at (a) the first, (b) the second, (c) the third, (d) the forth, (e) the fifth (closest) positions given in Table 1.

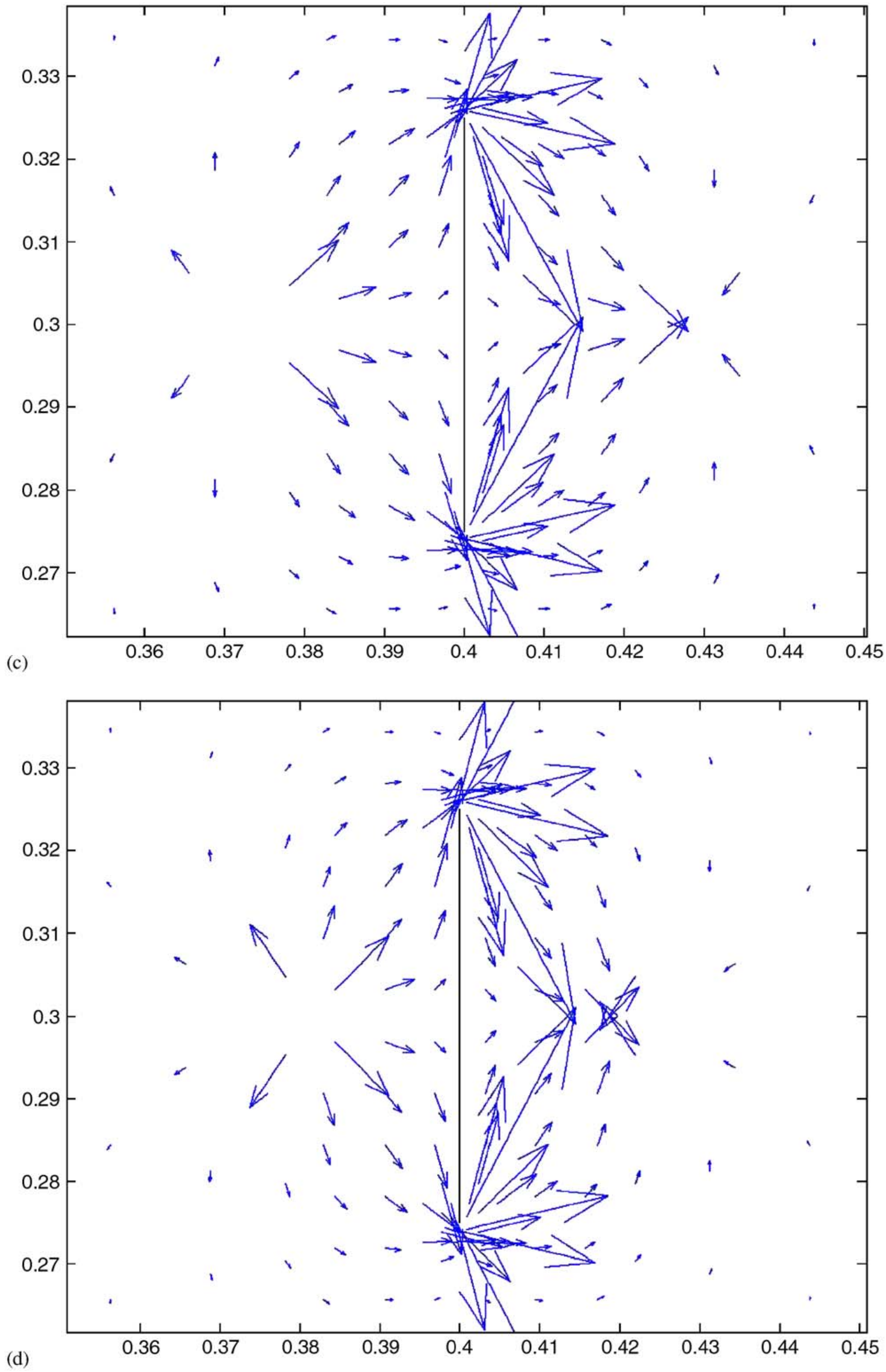

Fig. 7. (*Continued*)

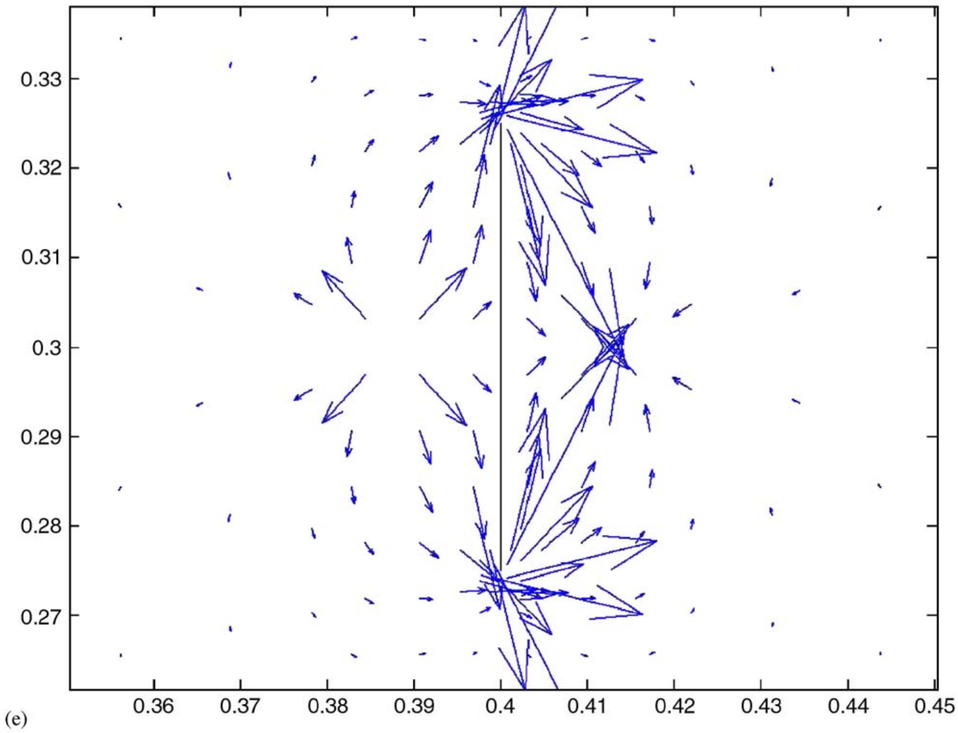

Fig. 7. (*Continued*)

from the source to the sink is nearly perpendicular to the crack, the presence of the flaw can be easily identified by the drastic changes in the flow pattern of the SI vectors near the crack.

The effect of the orientation of the crack with the direction of energy flow path is explored by changing the energy flow direction. Fig. 8 shows the SI around the crack when the source and the sink are positioned in line with the crack. For this type of orientation of the source and sink at this frequency, the presence of the crack could not be detected easily since the energy flow is parallel to the crack length. In the next case, the crack is assumed to be located horizontally to the length of the plate at the center of the plate. The SI of the plate with a horizontal crack is presented in Fig. 9. The alteration of the directions of SI vectors can be observed clearly in Fig. 10, which is an enlarged view around the crack. From the above investigations, it is found that the intensity vector must have one component that is perpendicular to the crack length for the crack to be easily detected.

The effects of crack length on the identification of the crack have been investigated by plate models with different crack lengths. In these simulations the cracks are between the sources and the sinks. Fig. 11 illustrates the SI vectors near a longer crack with a length of 10 cm and it can be seen that the presence of the crack is quite obvious. The SI field near a relatively short crack with a length of 1.25 cm is shown in Fig. 12. The changes of SI vectors around the crack are less obvious than that of a longer crack. The sizes of the element must be reduced more and more as the crack length is reduced and it will make it more difficult to detect the changes of flow pattern. To detect a smaller crack, the source and the sink need to be moved closer to the crack. Fig. 13 shows the SI vectors near the crack when the locations of the source and the sink are moved closer to the crack. It can be seen from the figure that the SI vectors are turning around the crack and the presence of a small crack can therefore be detected.

5.2. Diversion of energy flow near crack tips

In these simulations the strain energy release at the crack tip due to crack is considered. Dampers are attached at each tip of the crack representing the energy dissipation caused by strain energy released at the crack tip or the friction between the edges of the crack. The coefficients of damping of these dampers are taken

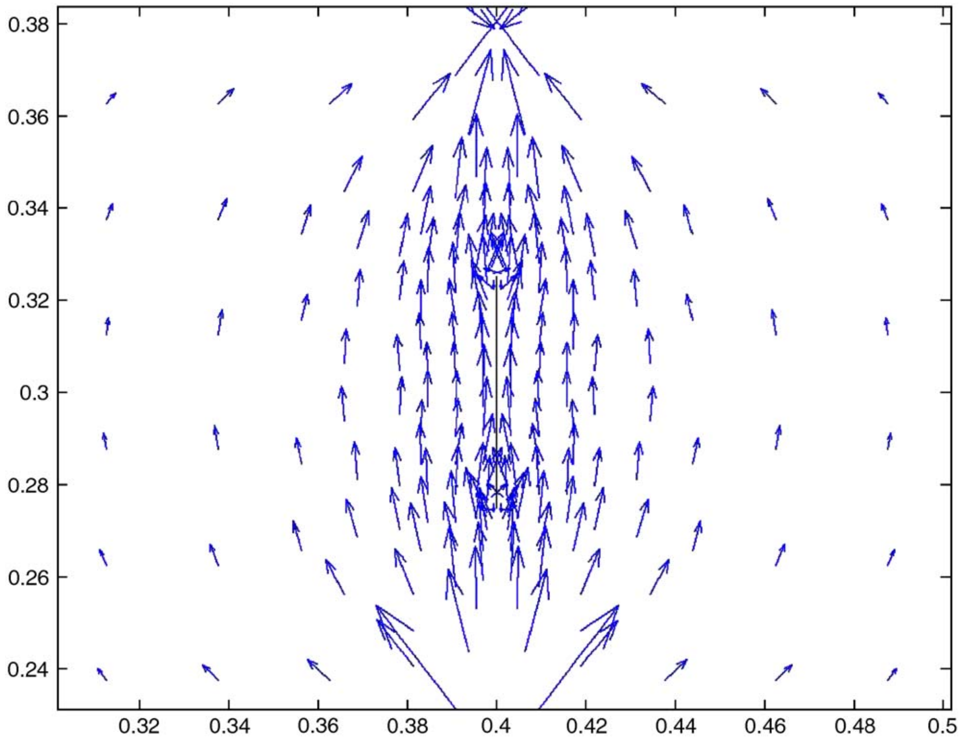

Fig. 8. Structural intensity around the crack; the source and the sink are vertically located and parallel to the line of crack.

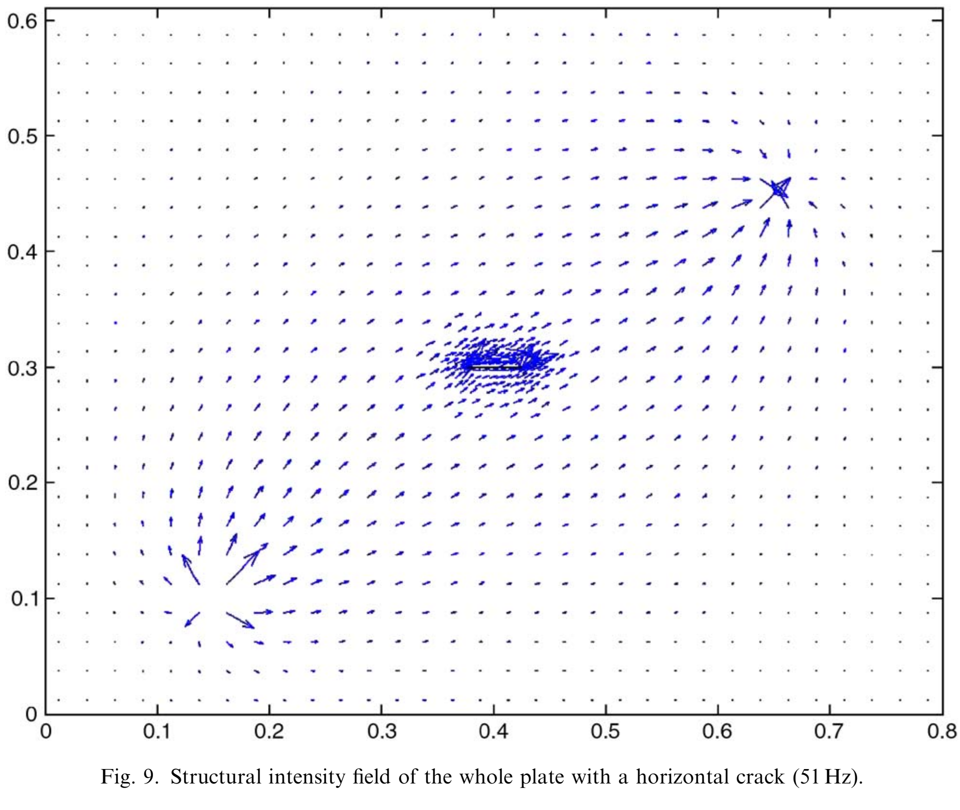

Fig. 9. Structural intensity field of the whole plate with a horizontal crack (51 Hz).

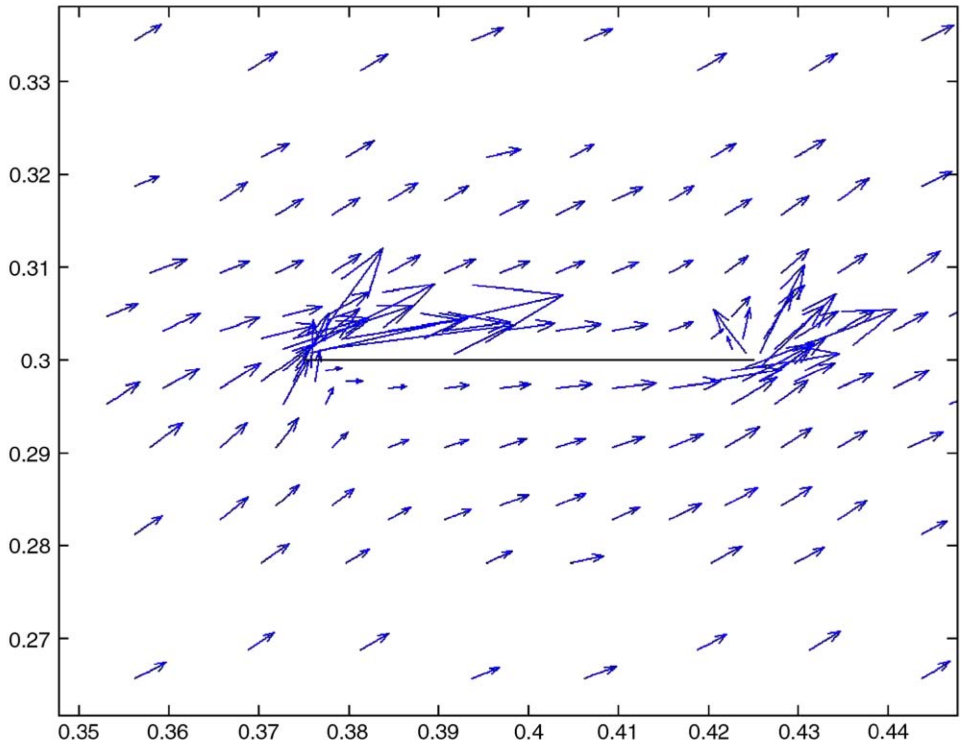

Fig. 10. An enlarged view of intensity vectors changing their direction at the crack.

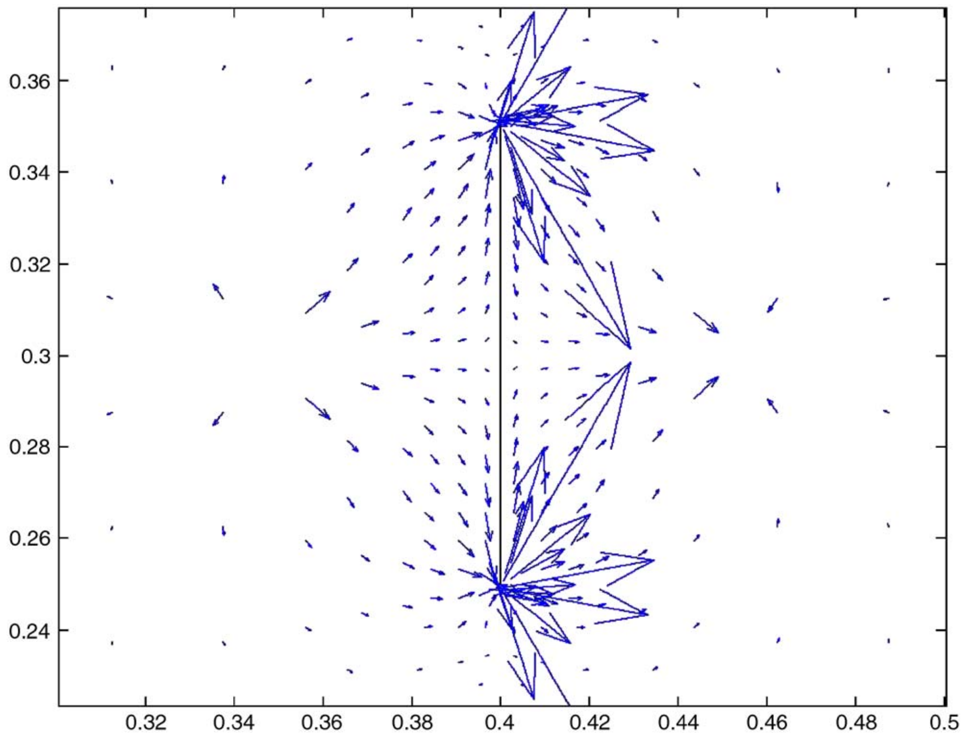

Fig. 11. Structural intensity vectors near a long crack.

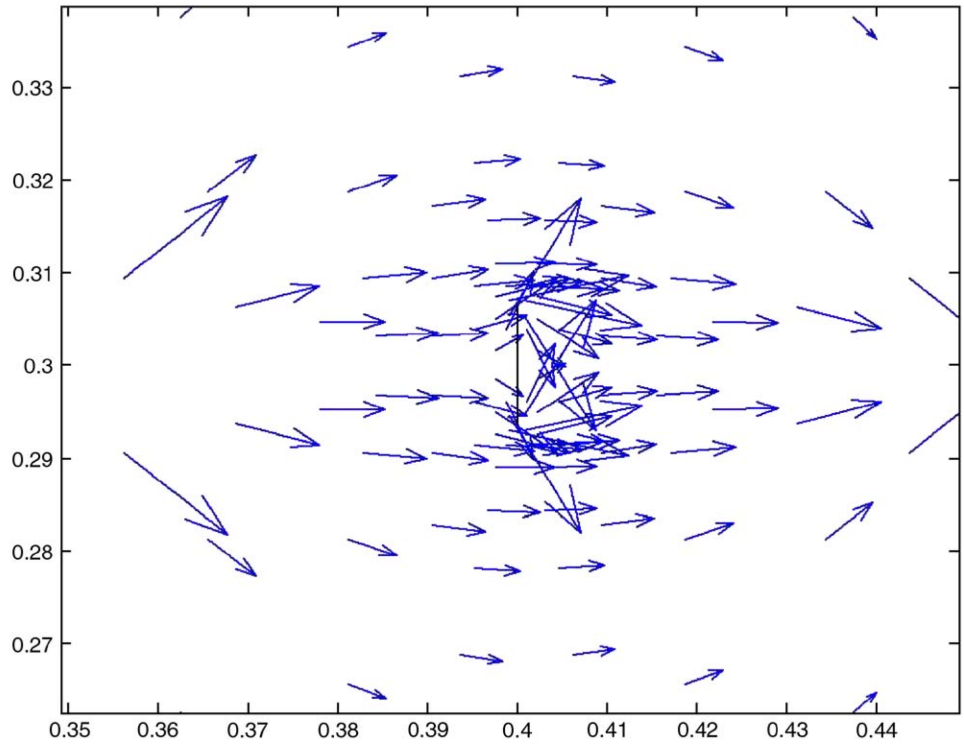

Fig. 12. Structural intensity vectors near a short crack.

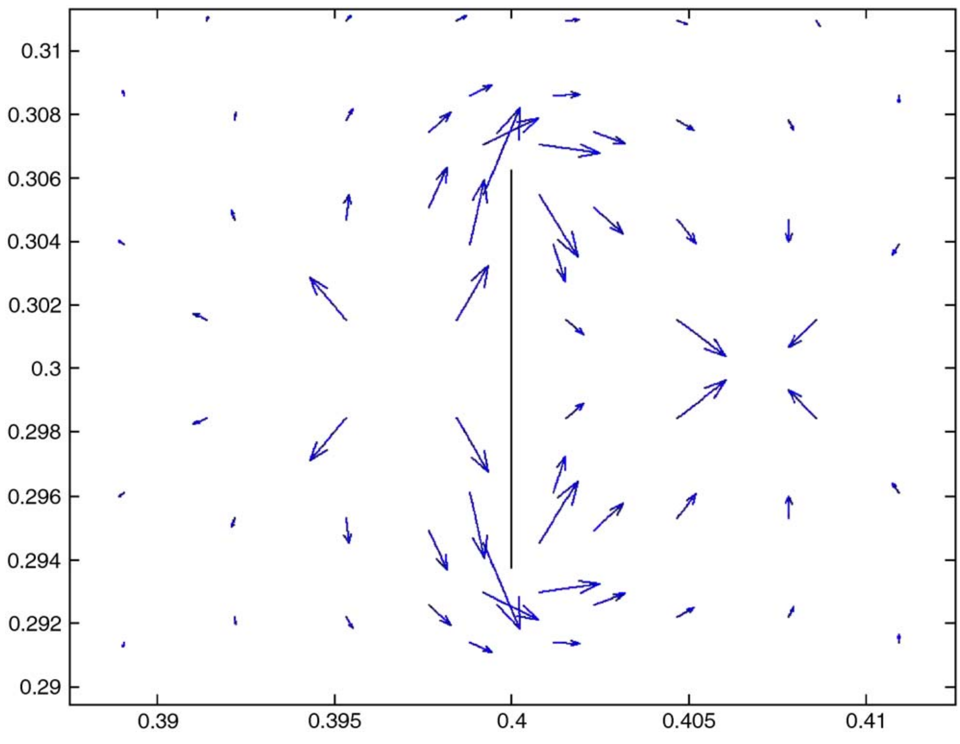

Fig. 13. Structural intensity vectors turning around a short crack when the source and the sink are very close to the crack.

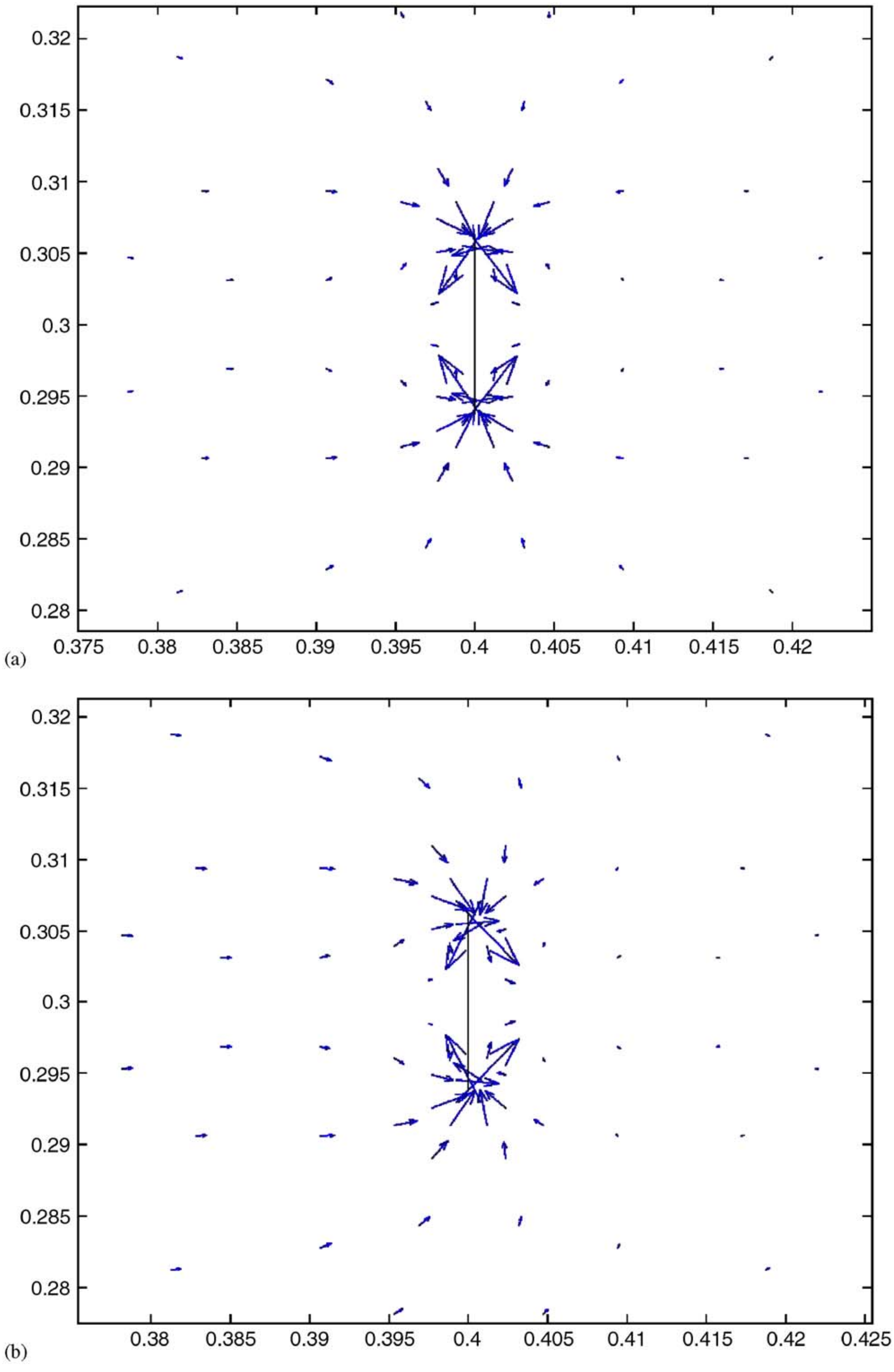

Fig. 14. SI field near the crack with energy dissipation at the crack tips (a) with no additional damper (b) an additional damper is attached at far field.

as 50 N s/m to demonstrate the idea and it is not intended to be representative of the actual energy release rate at the crack tips. Fig. 14(a) shows the SI around the crack with no presence of an additional damper. The energy dissipated at the crack tips serves as the energy sinks of the plate. When the additional damper with a

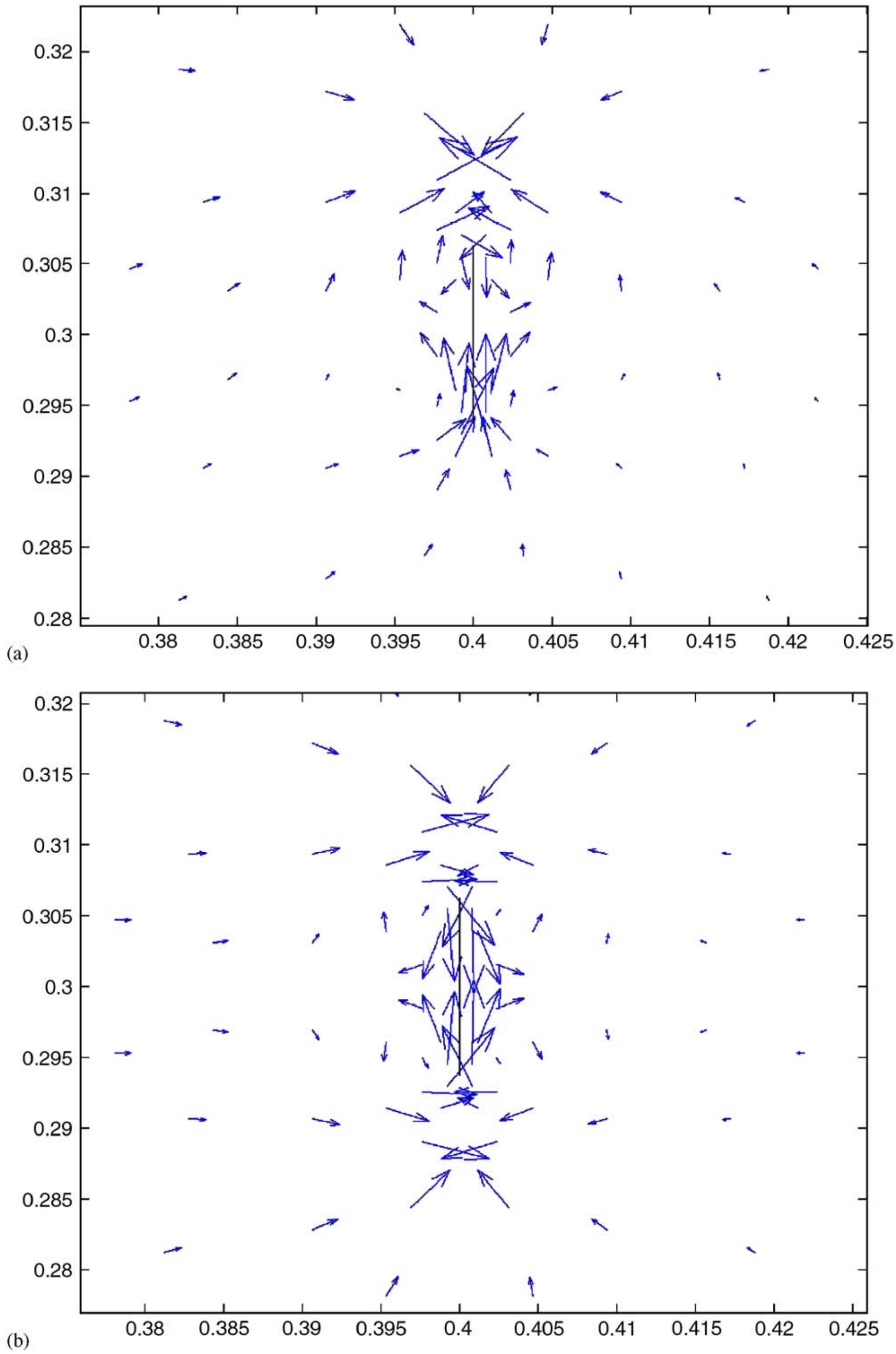

Fig. 15. SI field near the crack with energy dissipation at the crack tips and an additional damper is attached at far field (a) another damper is attached near the upper tip (b) two dampers are attached near both the upper and the lower tips.

damping coefficient of 900 N s/m is attached at a position far away form the crack, not much changes in SI vectors near the crack have been observed except for a little change in directions of intensity vectors occurring at the cracks tips as shown in Fig. 14(b).

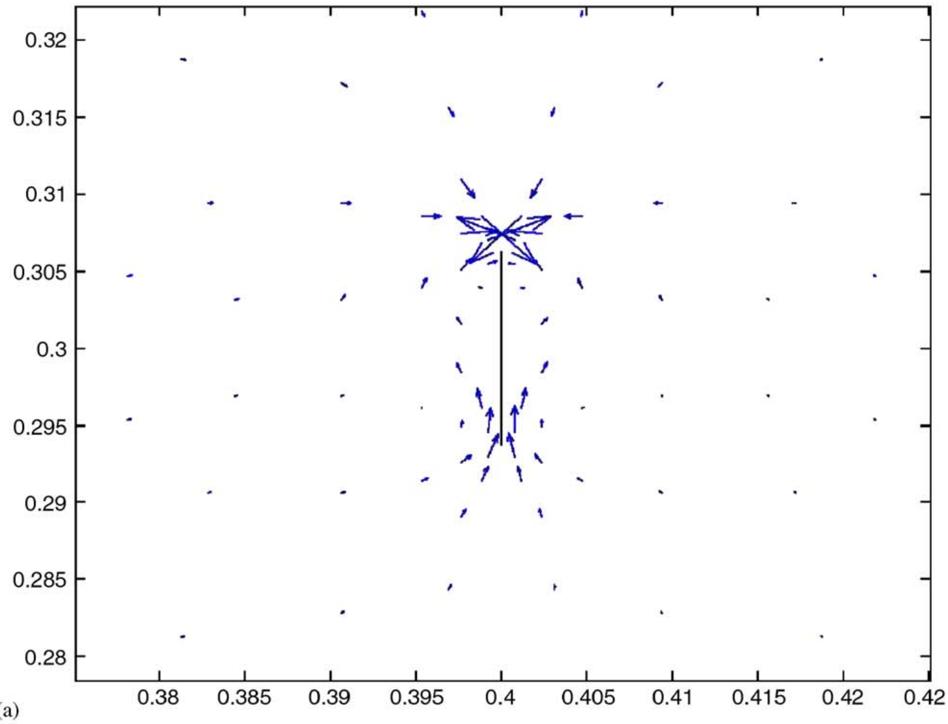

(a)

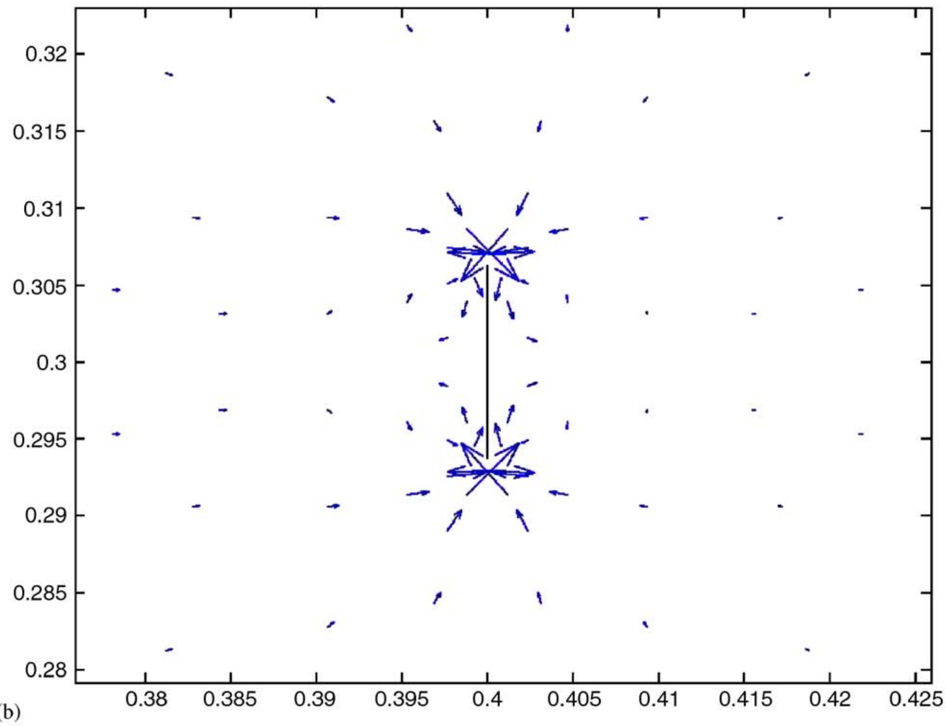

(b)

Fig. 16. SI field near the crack with energy dissipation at the crack tips and an additional damper is attached at far field (a) another damper is attached near the upper tip (b) two dampers are attached near both the upper and the lower tips.

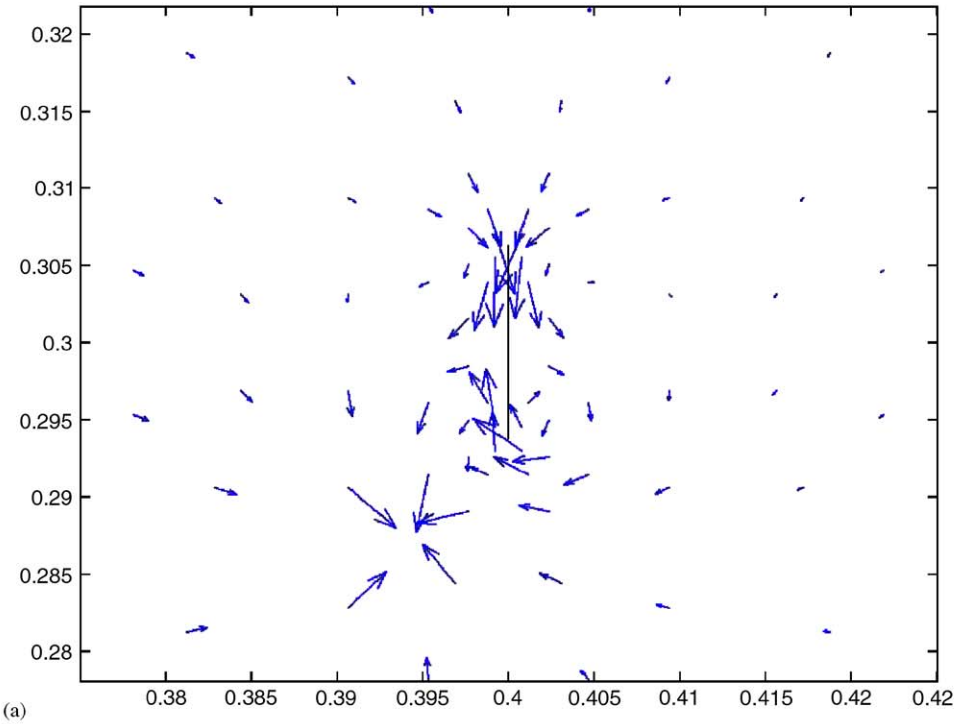

(a)

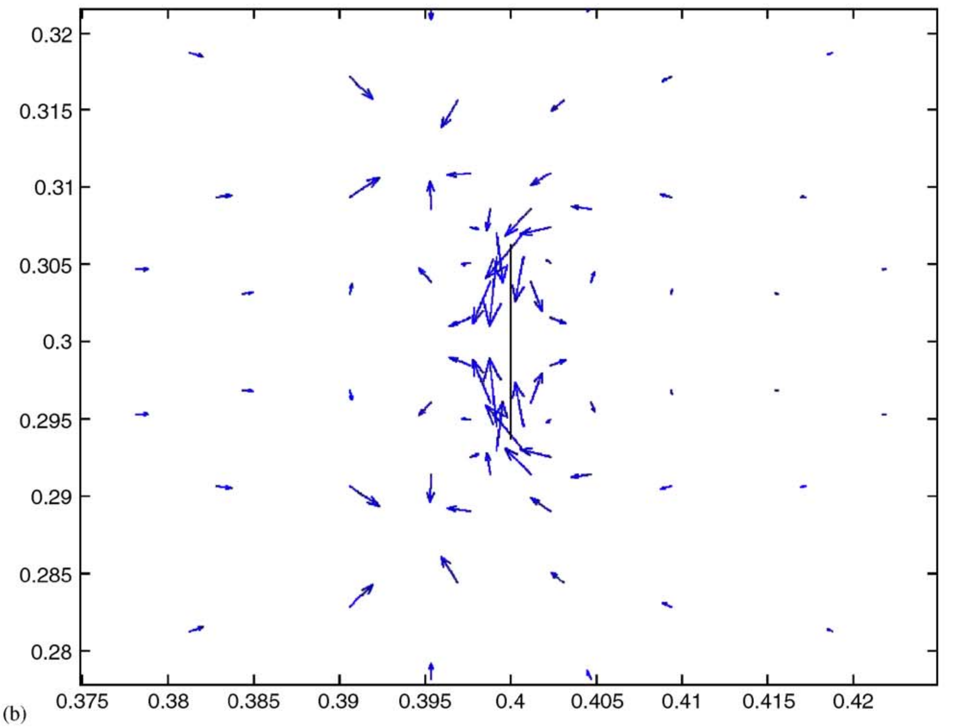

(b)

Fig. 17. SI field near the crack with energy dissipation at the crack tips and an additional damper is attached at far field (a) another damper is attached near the upper tip (b) two dampers are attached near both the upper and the lower tips.

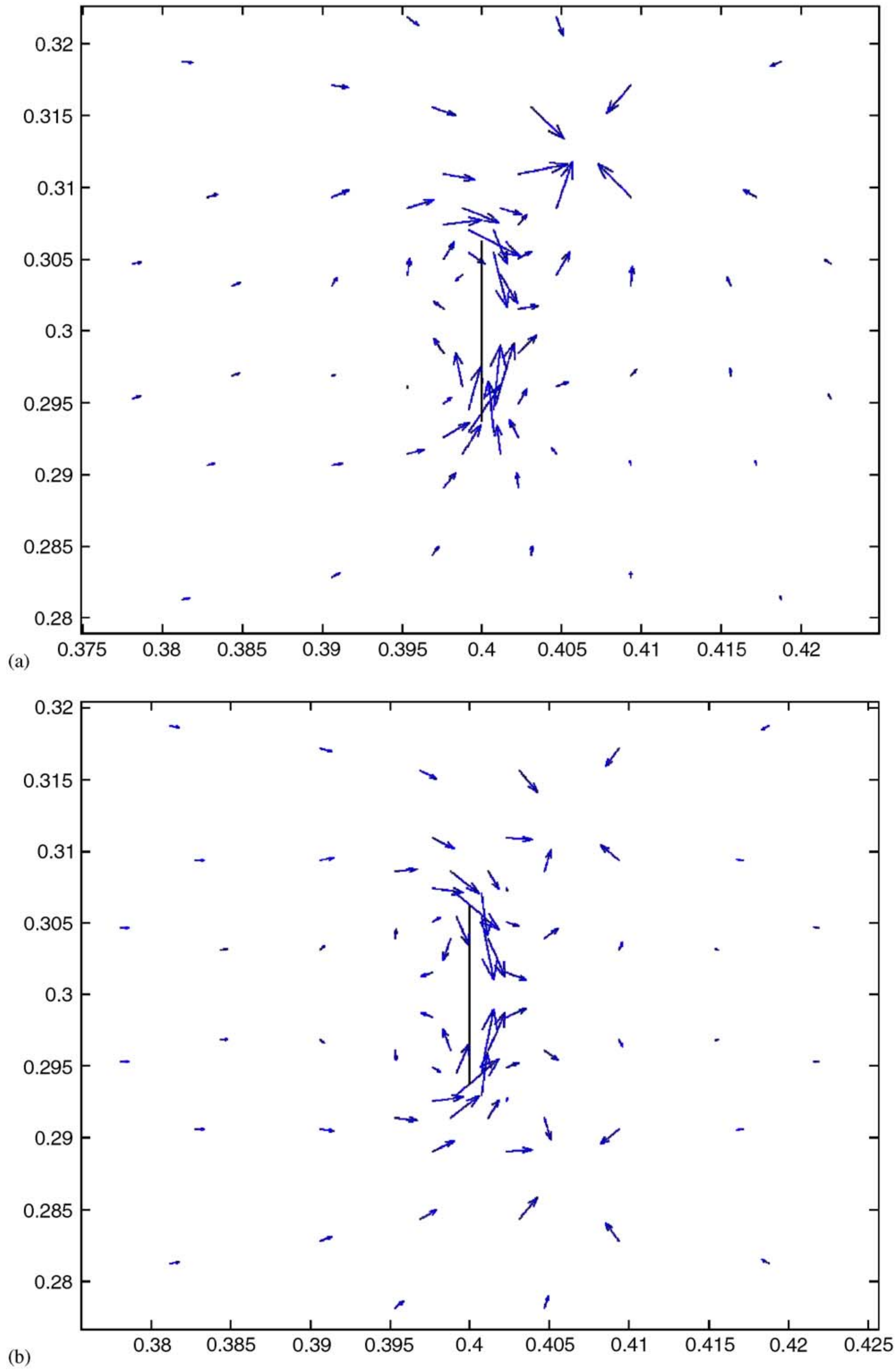

Fig. 18. SI field near the crack with energy dissipation at the crack tips and an additional damper is attached at far field (a) another damper is attached near the upper tip (b) two dampers are attached near both the upper and the lower tips.

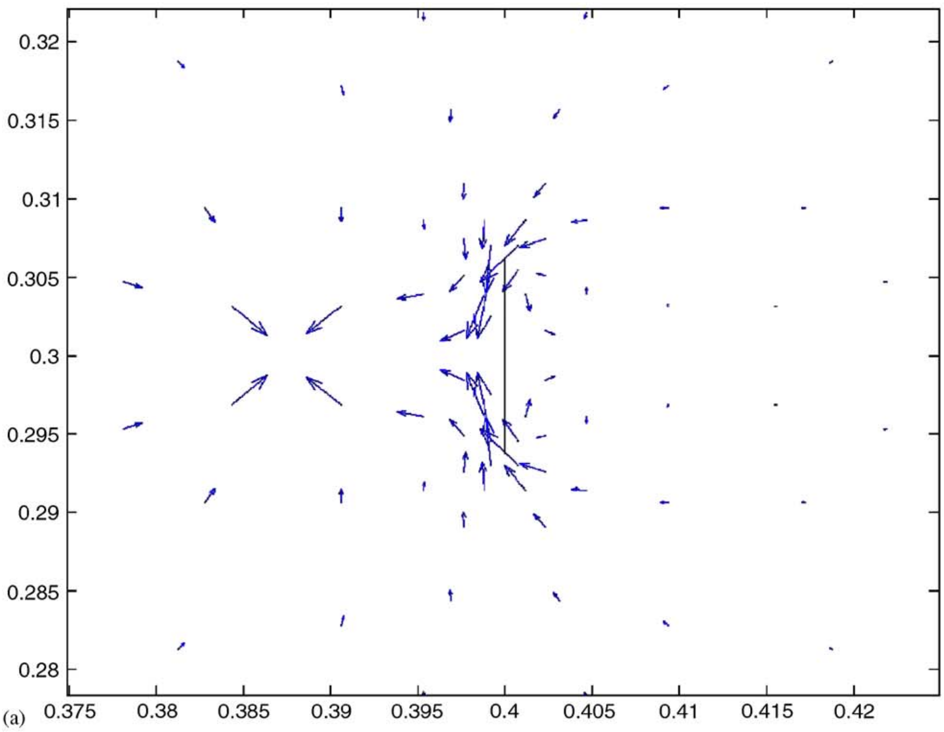

(a)

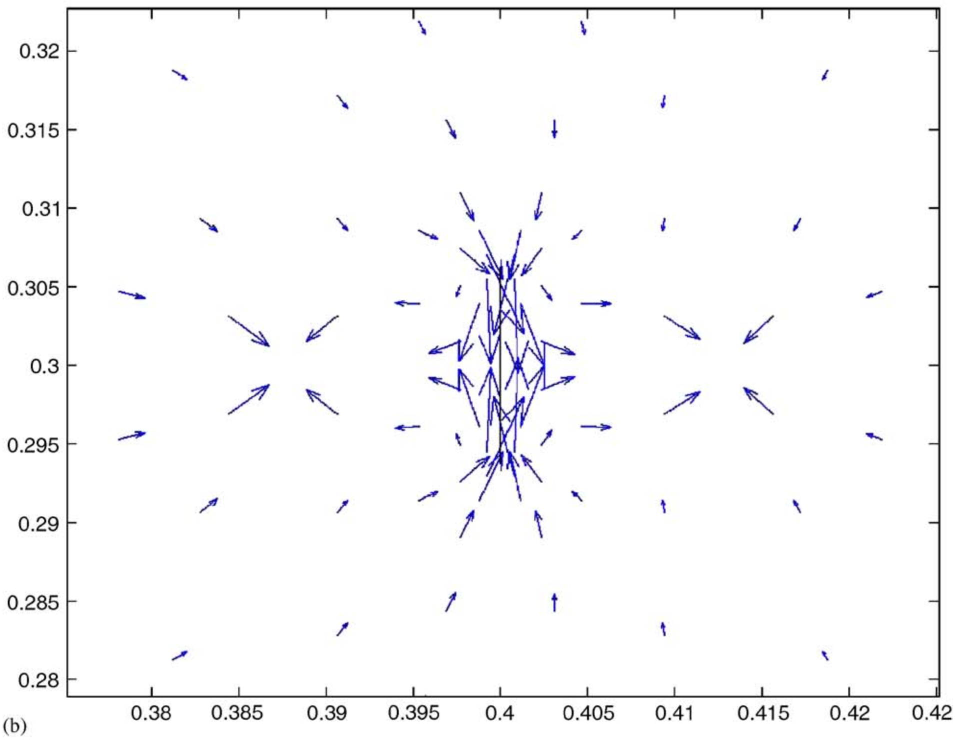

(b)

Fig. 19. SI field near the crack with energy dissipation at the crack tips and an additional damper is attached at far field (a) another damper is attached near the upper tip (b) two dampers are attached near both the upper and the lower tips.

Another additional damper having a damping coefficient of 2000 N s/m is attached near the upper tip of the crack in order to study the influence of additional energy dissipation on the crack tip. Fig. 15(a) shows the diversification of energy from the upper crack tip to the adjacent damper attached near it. The magnitude of SI at the upper tip is relatively smaller than that around the lower tip. In the next case the additional dampers are attached at directly above the upper tip and below the lower tip. The SI field near the crack is shown in Fig. 15(b). The additional dampers are moved closer to the crack tips and the results are shown in Figs. 16(a) and (b). The additional dampers are attached at the other locations around the crack and the results are shown in Figs. 17–19. According to the results, the diversion of dissipation of energy from the crack tip to the additional dampers can be observed.

It can therefore be concluded that proper positioning of suitable dampers near the crack tips in vibrating thin plates can be used to divert the vibrational energy flow away from crack tips. This approach can thus be used to protect the structure as a temporary measure before repair of the crack can be done. The SI technique can be used to assess the appropriateness of the locations and size of the dampers. The dampers can also be replaced by appropriate damping tapes or other damping devices in practical applications.

6. Conclusion

In this paper, the SI of a rectangular plate with a line crack is computed using the FEM. The presence of a flaw can be detected using the SI technique under certain circumstances. The horizontally located crack and vertically located crack as well as the effect of crack length are investigated. The flaw can be identified by the changes of energy flow pattern near its boundary. The detection of a relatively short crack is comparatively more difficult than that of a longer crack unless the source and the sink are moved closer to the crack. When the crack length is parallel to the energy flow, the detection of the crack is not feasible. The orientation of the crack relative to the energy flow path is essential for detecting the presence of the crack. The intensity vector must have one component that is perpendicular to the crack length to detect the presence of the crack. It is also found that proper positioning of dampers near the crack tips in vibrating thin plates can be used to divert the vibrational energy flow away from crack tips, thus to protect them as a temporary measure before repair of the crack can be done. SI technique can be used to assess the appropriateness of the locations and size of the dampers.

References

[1] S.E. Khadem, M. Rezaee, An analytical approach for obtaining the location and depth of an all-over part-through crack on externally in-plane loaded rectangular plate using vibration analysis, *Journal of Sound and Vibration* 230 (3) (2000) 291–308.

[2] A.D. Dimarogonas, Vibration of cracked structures: a state of the art review, *Engineering Fracture Mechanics* 55 (5) (1996) 831–857.

[3] B. Stahl, L.M. Keer, Vibration and stability of cracked rectangular plates, *International Journal of Solids and Structures* 8 (1972) 69–91.

[4] H.P. Lee, Fundamental frequencies of annular plates with internal cracks, *Computers and Structures* 43 (6) (1992) 1085–1089.

[5] R. Solecki, Bending vibration of a simply supported rectangular plate with a crack parallel to one edge, *Engineering Fracture Mechanics* 18 (6) (1983) 1111–1118.

[6] M. Krawczuk, A. Zak, W. Ostachowicz, Finite element model of plate with elasto-plastic through crack, *Computers and Structures* 79 (2001) 519–532.

[7] D.U. Noiseux, Measurement of power flow in uniform beams and plates, *Journal of the Acoustical Society of America* 47 (1970) 238–247.

[8] G. Pavic, Measurement of structure borne wave intensity—part I: formulation of the methods, *Journal of Sound and Vibration* 49 (2) (1976) 221–230.

[9] J.W. Verheij, Cross spectral density methods for measuring structure borne power flow on beams and pipes, *Journal of Sound and Vibration* 70 (1) (1980) 133–138.

[10] S.A. Hambric, Power flow and mechanical intensity calculations in structural finite element analysis, *Journal of Vibration and Acoustics* 112 (1990) 542–549.

[11] L. Gavric, G. Pavic, A finite element method for computation of structural intensity by the normal mode approach, *Journal of Sound Vibration* 164 (1) (1993) 29–43.

[12] Y.J. Li, J.C.S. Lai, Prediction of surface mobility of a finite plate with uniform force excitation by structural intensity, *Applied Acoustics* 60 (2000) 371–383.

[13] T.Y. Li, W.H. Zhang, T.G. Liu, Vibrational power flow analysis of damaged beam structures, *Journal of Sound and Vibration* 242 (1) (2001) 59–68.
[14] M.S. Khun, H.P. Lee, S.P. Lim, Computation of structural intensity for plates with multiple cutouts, *Structural Engineering and Mechanics* 16 (5) (2003) 627–641.
[15] X.D. Xu, H.P. Lee, C. Lu, Numerical study on energy transmission for rotating hard disk systems by structural intensity technique, *International Journal of Mechanical Sciences* 46 (2004) 639–652.
[16] X.D. Xu, H.P. Lee, C. Lu, The structural intensities of composite plates with a hole, *Composite Structures* 65 (2004) 493–498.
[17] X.D. Xu, H.P. Lee, Y.Y. Wang, C. Lu, The energy flow analysis in stiffened plates of marine structures, *Thin Wall Structures* 42 (2004) 979–994.
[18] N.K. Anifantis, Crack surface interface: a finite element analysis, *Engineering Fracture Mechanics* 68 (2001) 1403–1415.
[19] L. Banks-Sills, Y. Bortman, Reappraisal of the quarter-point quadrilateral element in linear elastic fracture mechanics, *International Journal of Fracture* 25 (1984) 169–180.
[20] J.G. Malone, P.G. Hodge Jr., R. Plunkett, Finite element mesh for a complete solution of a problem with a singularity, *Computers and Structures* 24 (4) (1986) 613–623.
[21] A. Vafai, H.E. Estenkanchi, A parametric finite element study of cracked plates and shells, *Thin-Walled Structure* 33 (1999) 211–229.
[22] *ABAQUS User's Manuals*, Version 6.2-1, Hibbitt, Karlsson and Sorensen, Inc., USA, 2001.